



Corrosion Resistance of Niobium-Coated Carbon Steel

Paloma Detlinger¹ · Brian Utri¹ · Everson do Prado Banczek¹

Received: 23 February 2018 / Revised: 18 October 2018 / Accepted: 13 November 2018 / Published online: 21 November 2018
© Springer Nature Switzerland AG 2018

Abstract

In this work, the effectiveness of niobium coatings for the corrosion protection of carbon steel was studied. Three niobium resins, containing different molar proportions of citric acid:ethylene glycol, were coated separately onto samples of carbon steel (SAE 1020). The niobium layers were obtained by the polymeric precursor method (Pechini). Potentiodynamic polarization curves (anodic and cathodic) and electrochemical impedance spectroscopy were used to evaluate the corrosion resistance of the niobium-coated carbon steel samples in a 0.5 mol L⁻¹ NaCl electrolyte solution. X-ray diffraction analysis of the niobium layers showed that they are composed of the niobates: NbO, NbO₂ and Fe_{0.998}Nb_{0.002}. Surface observation by scanning electron microscopy revealed a uniformly deposited niobium coating on the surface. The electrochemical results showed that niobium was effective in the corrosion protection of the carbon steel substrate. The results also suggested that niobium can be coated onto the substrate to form a layer with advantageous corrosion properties.

Keywords Pechini method · Corrosion · Niobium ammonium oxalate

1 Introduction

Niobium oxides exhibit high corrosion resistance in corrosive environments such as wet or dry chlorine, bromine, saturated brine, ferric chloride, hydrogen, sulfide, sulfur dioxide, nitric and chromic acids, and sulfuric and hydrochloric acids within the specified temperature range and concentration [1].

Surface treatments are used for metal corrosion protection; however, due to the toxicity problems generated with the use of these traditional treatments, niobium oxides arise as an alternative since their biocompatibility and efficiency as a corrosion protector are already proven [2, 3].

Niobium oxide films have been widely studied for corrosion protection of various metallic materials due to their high resistance to corrosion, mechanical resistance, and

biocompatibility [4–9]. Niobium coatings can be obtained by (i) hydrothermal synthesis [4–6], co-precipitation synthesis [7, 8] (ii) the sol–gel technique [9–14] and (iii) the Pechini method [9, 15–18].

The Pechini method, or polymeric precursor method, is a modification of the sol–gel method that consists of the preparation of a resin with the desired metal complexed to the structure and calcinating it to form metallic oxides [19, 20]. The resin is prepared by reacting a chelating agent (usually a carboxylic acid) and the metallic precursor (usually a salt), followed by a polyesterification reaction by the addition of a polyalcohol [19–23]. This method stands out for the possibility to control the particle size, morphology and compositional homogeneity as well as a low toxicity and relatively moderate conditions of temperature, besides allowing production in large scale at relatively low costs [19–25].

Niobium oxides are commonly found as NbO, NbO₂ and Nb₂O₅, where the element Nb has the oxidation state +2, +4 and +5, respectively [26]. NbO crystallizes as a face-centered cube and is considered as a conductor [21, 26]. NbO₂ crystallizes in the tetragonal phase and is considered as a semiconductor [21, 26]. Nb₂O₅ is the most thermodynamically stable state and can occur in the amorphous state or as different polymorphs (hexagonal, orthorhombic or monoclinic) depending of the crystallization temperature [26]. Nb₂O₅ is considered

✉ Everson do Prado Banczek
edopradobanczek@yahoo.com.br

Paloma Detlinger
PalomaDetlinger@hotmail.com

Brian Utri
brian_utri@hotmail.com

¹ Departamento de Química, Universidade Estadual do Centro-Oeste, UNICENTRO, Rua Simeão Varela de Sá, 03, Guarapuava, PR CEP 85040-080, Brazil

as an insulant, therefore, it would be the ideal structure for the corrosion protection.

The variation in molar ratio between citric acid and ethylene glycol in the formation of niobium oxide films by the Pechini method has a great influence on the degree of polymerization. Films prepared with a high molar ratio of citric acid to ethylene glycol showed a crystalline structure, while those prepared a low ratio of the reactants have amorphous structures [13].

Raba et al. [27] carried out a comparative study between the sol-gel and Pechini methods for the preparation of Nb₂O₅ powders. According to analyses made using scanning electron microscopy (SEM), the average size of the grains formed using the Pechini method was lower than that of grains obtained by the sol-gel method. In addition, it was demonstrated that the size of the grains formed by the sol-gel method is less uniform.

Rincón et al. [28] investigated the resistance to corrosion of a niobium carbide (NbC)-based coating applied on AISI 1045 steel, using 3% NaCl solution as the electrolyte. The results indicated that the presence of NbC increased the corrosion resistance of the substrate, but there was a decrease in protection after exposure to the solution for 24 h. This decrease was attributed to the porosity of the coating.

Fernandes et al. [29] studied an NbC coating applied on AISI 52100 steel, which is used in machine bearings. This coating increased the corrosion resistance of the material, in addition to increasing the mechanical strength of the metal.

The objective of this work was to produce and characterize a niobium-based coating for corrosion protection of carbon steel (SAE 1020) by varying the molar ratio of citric acid (CA) to ethylene glycol (EG) in the niobium resin.

2 Experimental

2.1 Sample Preparation

The material used as substrate was a carbon steel (SAE 1020) (composition in Table 1), from which samples (20×20×2 mm) were cut and then coated with niobium.

The sample surfaces were prepared for niobium coating by grinding with silicon carbide (SiC) emery paper in the sequence #220, #320, #400, #600 and #1220. After grinding, the samples were rinsed with distilled water to remove any residual impurities, and dried. The polished plate was immersed in the resin for 15 min, then hanged to drain the excess of resin for 5 min followed by the calcination of the plates at 450 °C for 1 h in a preheated muffle furnace [19]. After calcination the plates were cleaned with a soft paint

Table 1 Percentage composition of carbon steel alloy (1020), obtained by X-ray fluorescence

Element	Fe	Mn	C
(%)	99.12	0.32	0.20

brush, rinsed with deionized water and dried to remove the organic material left.

The three resins were proposed to evaluate the effect of ethylene glycol on the corrosion protection promoted by the niobium coating (Table 2). Films prepared with a high molar ratio of citric acid to ethylene glycol showed a crystalline structure, while those prepared a low ratio of the reactants have amorphous structures [13].

The niobium coatings preparation and characterization of the metal samples followed the sequence of Fig. 1.

The resins for carbon steel coating were prepared by the Pechini method [19], using the following reagents: ethylene glycol (99.99%, Aldrich), citric acid (99.999%, Aldrich), and complex ammonium nitrate (NH₄)₃(NbO (C₂O₄)₃)·H₂O.

2.2 Characterization of the Niobium Layers

The morphology of the niobium coatings was evaluated by SEM using a Tescan® Vega3 microscope, and their thickness was determined by thickness measurements at

Table 2 Molar ratio EG/CA for resin preparation

Resin	Molar ratio		
	Ethylene glycol	Citric acid	Nb: citric acid
1	4	1	1:10
2	8	1	1:10
3	12	1	1:10

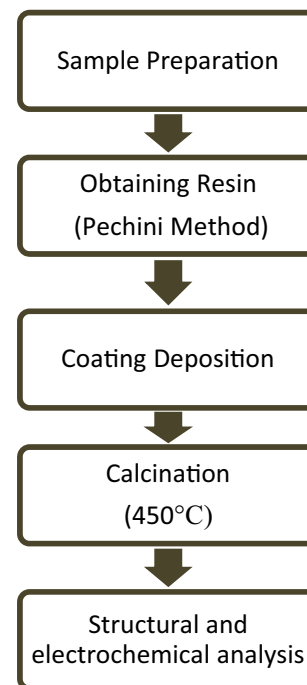


Fig. 1 Stages of preparation of the samples and resins used

ten areas of the three different samples. The phases in the niobium layer were investigated by XRD with a Bruker D2 phaser diffractometer, using $\text{CuK}\alpha$ radiation (1.5418 \AA). The electrochemical behavior of the niobium-coated samples was evaluated by potentiodynamic polarization (anodic and cathodic) measurements and electrochemical impedance spectroscopy (EIS), using a frequency response analyzer (Gamry model EIS 300) coupled to a potentiostat PCI4/300. Working electrodes with an area of 0.78 cm^2 were used in the electrochemical tests. A platinum wire and a silver/silver chloride electrode were used as the counter and reference electrodes, respectively. A sodium chloride solution ($0.5 \text{ mol L}^{-1} \text{ NaCl}$; pH 6.0) was used for electrochemical characterization of the niobium layer. The electrolyte was quiescent, naturally aerated and its temperature was maintained at $(20 \pm 2) \text{ }^\circ\text{C}$. Potentiodynamic polarization tests were carried out from the corrosion potential E_{corr} up to an overpotential of $\pm 400 \text{ mV}$, using a scanning rate of 1 mV s^{-1} . The EIS measurements were potentiostatically performed at E_{corr} , with a perturbation amplitude of $\pm 10 \text{ mV rms}$, in the frequency range from 100 kHz to 10 mHz , using an acquisition rate of 10 points per decade. The configuration of the electrochemical cell used is shown in Fig. 2.

Corrosion rates (j_{corr}) were estimated by extrapolation of the linear segment of the cathodic curve to the corrosion potential. The average corrosion potential (E_{corr}) and (j_{corr}) values are estimated from three measurements. The corrosion inhibiting efficiency (θ) was estimated by

$$\theta = \frac{j_{\text{corr}}^0 - j_{\text{corr}}}{j_{\text{corr}}^0}, \quad (1)$$

where j_{corr}^0 is the corrosion rates of substrate. j_{corr} is the corrosion rates of coated substrate.

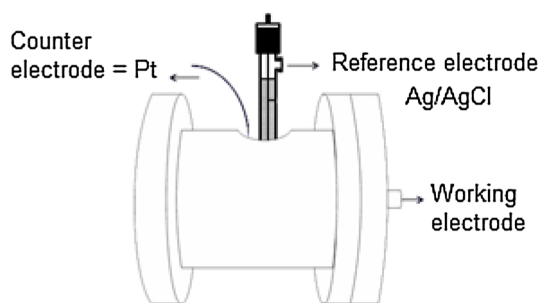


Fig. 2 Schematic model of the electrolytic cell used in electrochemical tests

3 Results and Discussion

3.1 Characterization of Phases in the Niobium Coating

The phases in the niobium layers obtained with different types of resin were analyzed by XRD and the results are shown in Fig. 3.

The X-ray diffractogram in Fig. 3a shows that the powder formed by the resin has an amorphous structure. However, when the resin is applied on carbon steel (SAE 1020), it was possible to identify characteristic niobium oxide peaks. The presence of carbon steel induces phase formation, since the diffractogram of niobium coated on carbon steel presents well-defined peaks, characteristic of crystalline material (Fig. 3b). The phases present in the carbon steel niobium coating were mainly NbO , NbO_2 and $\text{Fe}_{0.998}\text{Nb}_{0.002}$ [30].

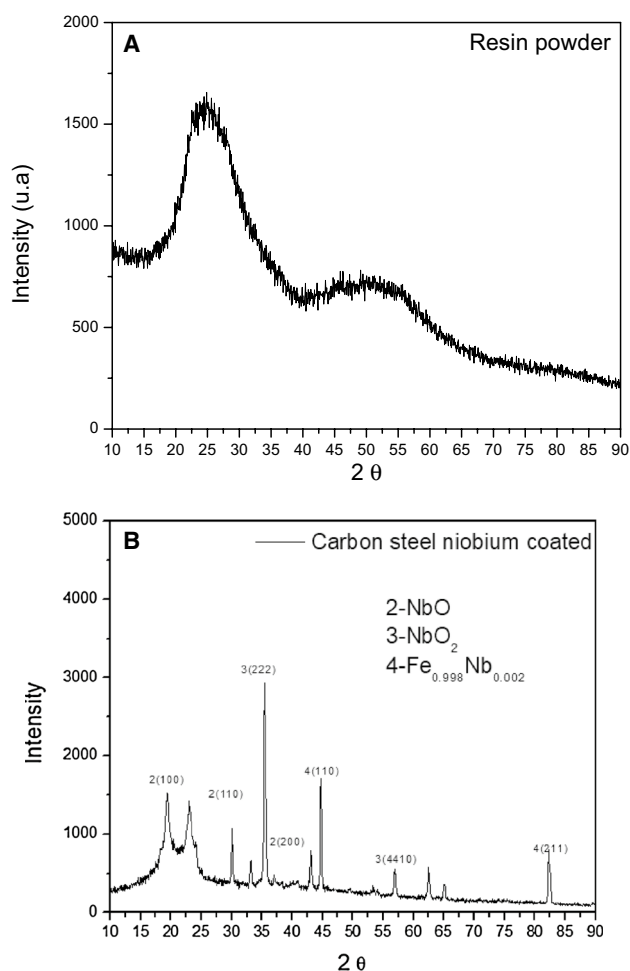


Fig. 3 X-ray diffractogram of the **a** resin powder and **b** carbon steel (SAE 1020) niobium coating

3.2 Morphology Characterization of the Niobium Coating

The niobium coating morphology was evaluated by SEM and the micrographs obtained are shown in Fig. 4.

Coating of carbon steel promotes considerable change in the surface morphology of the substrate. The coatings obtained with the niobium resins 1, 2 and 3, show a granular morphology that promotes surface coverage. This suggests that the niobium layer leads to better corrosion resistance.

Different niobium resins resulted in different coating characteristics. The coating obtained with resin 1 was the most homogeneous and compact. That obtained with resin 2 showed some defects, such as cracks and pores. The coating obtained with resin 3 showed a morphology with smaller crystals. The micrographs suggest that the increasing sequence of corrosion protection is resin 1 > resin 3 > resin 2. This corrosion protection sequence is related to the morphology of the niobium layers, as the coating of resin 1 was the most homogeneous and compact.

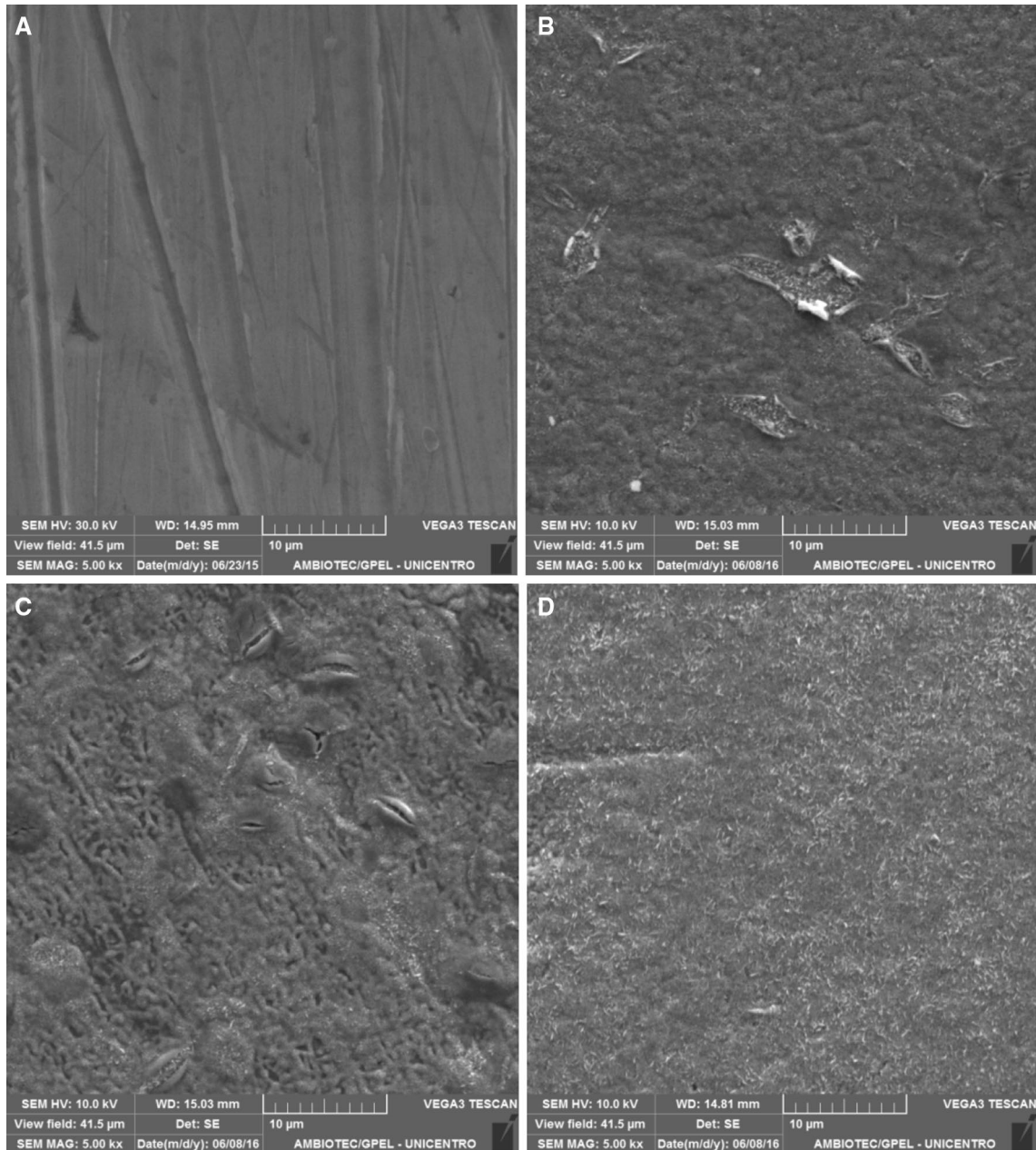


Fig. 4 Micrographs of the carbon steel (SAE 1010) surface prior to niobium coating (a) and after niobium coating with resin 1 (b), resin 2 (c) and resin 3 (d)

The semi-quantitative elemental compositions obtained from energy dispersive spectroscopy (EDS) analysis of the niobium coatings are shown in Table 3.

The EDS results show that the niobium layers contain mainly iron, niobium, and carbon. The high amount of iron is mainly due to the metallic substrate. Coating the carbon steel with niobium decreases the amount of iron determined on the surface of the carbon steel. The presence of carbon shows that there was incomplete burning of the resin organic fraction in the calcination step. The smaller amount of niobium present in the resin coating 3 suggests that this layer is composed of iron oxide.

The amount of niobium varied considerably with the proportion of ethylene glycol used in each resin. The substrate coated with resin 1 presented the highest percentage of niobium in its coating composition (Fig. 5).

The niobium percentage in the coating decreases with increasing ethylene glycol ratio; the higher the amount of ethylene glycol, the lower the amount of citric acid complexing agent. According to Galceran et al. [31], a very small molar ratio of citric acid to ethylene glycol can lead to precipitation of niobium salts and non-uniformity in the complexation reaction. A smaller amount of citric acid decreases the amount of niobium complexed by citric acid and favors the precipitation of niobium salts by decreasing the amount of niobium in the coating. The results are in agreement with the study carried out by Rosário and Pereira [16], which concluded that niobium-based films prepared with a citric acid:ethylene glycol molar ratio of 1:4 provide the best corrosion protection.

3.3 Niobium Layer Thickness Evaluation

The niobium layer thickness was evaluated by means of SEM on cross-sectional areas of coated steel, as shown in Fig. 6. The mean thickness value for the niobium layer was $14.93 \pm 0.997 \mu\text{m}$.

These results are in agreement with the literature [3, 32]. Tussolini [32] measured the thickness of the niobium-based coatings and found values of $(20 \pm 2) \mu\text{m}$. Castillejo et al. [33] also measured the thickness of their niobium-based coatings and the dimensions established were $15 \pm 0.4 \mu\text{m}$.

Table 3 Semi-quantitative elemental compositions of niobium layers obtained with different resins

Sample	Element (wt%)			
	C	O	Fe	Nb
Carbon steel (SAE 1020)	4.59	–	95.1	–
Carbon steel (SAE 1020) + resin 1	2.00	21.5	66.0	10.5
Carbon steel (SAE 1020) + resin 2	1.96	21.3	68.1	8.64
Carbon steel (SAE 1020) + resin 3	1.52	20.8	77.7	0.07

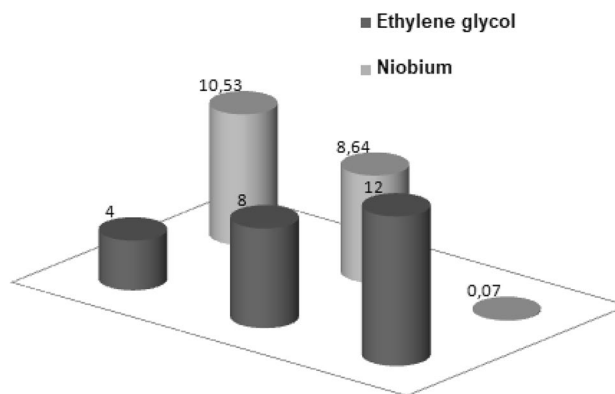


Fig. 5 Niobium percentage variation as a function of ethylene glycol proportion in the resin

3.4 Electrochemical Characterization

The anodic polarization curves corresponding to bare and niobium-coated carbon steel samples are shown in Fig. 7.

Lower current densities were measured for niobium-coated samples up to potential values of -0.5 V , suggesting that the coated samples were protected against corrosion in the region near corrosion potential. At potential values greater than -0.5 V , there was rupture of the niobium coatings indicated by the significant increase in current density when compared to uncoated carbon steel.

The anodic polarization results demonstrated that the niobium coatings protect the metal surface, but it is not possible to define the best coating because the measured current densities were very close to all coatings. These

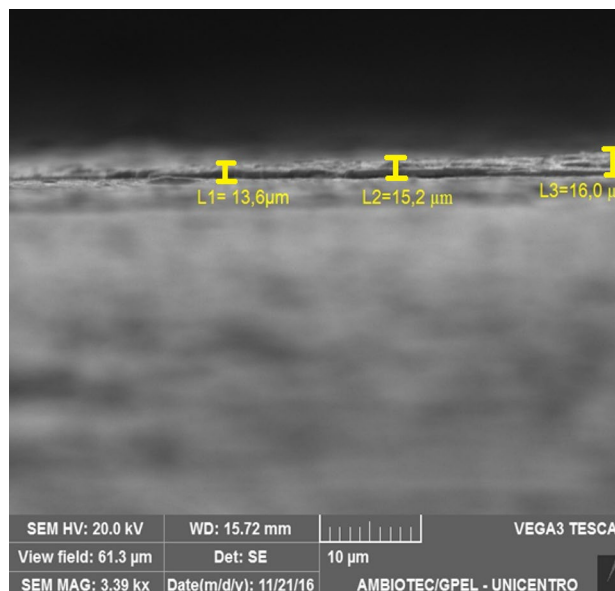


Fig. 6 Cross-section of the niobium-coated carbon steel (SAE 1020) showing the thickness of the niobium layer

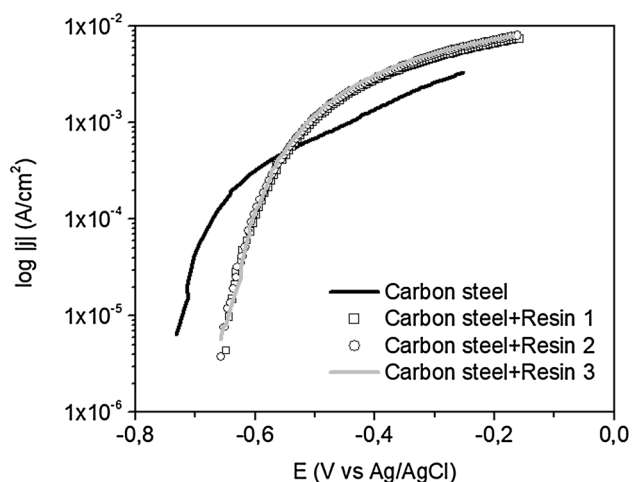


Fig. 7 Anodic polarization curves of bare and niobium-coated carbon steel (SAE 1010), obtained in NaCl 0.5 mol L⁻¹ solution

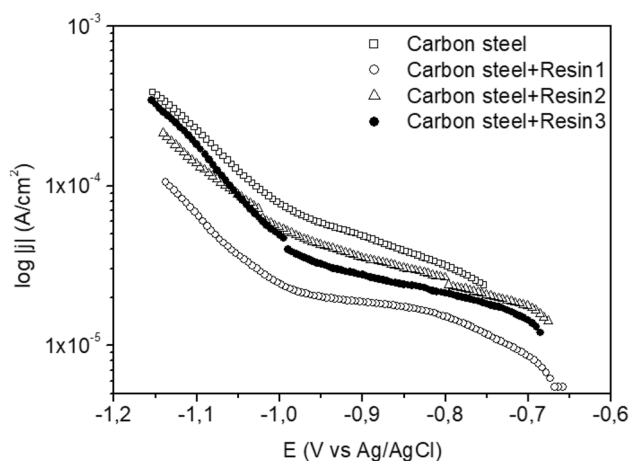


Fig. 8 Cathodic polarization curves of bare and niobium-coated carbon steel (SAE 1020), obtained in NaCl 0.5 mol L⁻¹ solution

results showed that in the anodic polarization the differences in morphology and structure were not enough to determine a change of electrochemical response.

Cathodic polarization curves were also obtained in NaCl 0.5 mol L⁻¹ solution, and these are shown in Fig. 8.

For all cathodic polarization curves, a current density limit (j_L) was observed, showing that the cathodic reaction is diffusion controlled. The j_L values decreased for the niobium-coated steels compared to the bare steel, and the lowest j_L value was associated with the resin 1 niobium-coated steel, indicating that the layer polarized the cathodic reaction.

From the results of cathodic polarization, it was observed that the electrochemical response demonstrates that the niobium coating acts of the oxygen reduction

Table 4 Average values of j_{corr} , E_{corr} and efficiency (θ) obtained from cathodic polarization curves

Sample	E_{corr} (V)	j_{corr} ($\mu\text{A cm}^{-2}$)	θ (%)
Carbon steel	-0.75 ± 0.03	39.7	–
Carbon steel + resin 1	-0.65 ± 0.05	11.6	70.8 ± 2.5
Carbon steel + resin 2	-0.68 ± 0.09	23.0	42.1 ± 1.8
Carbon steel + resin 3	-0.69 ± 0.04	20.4	48.6 ± 1.5

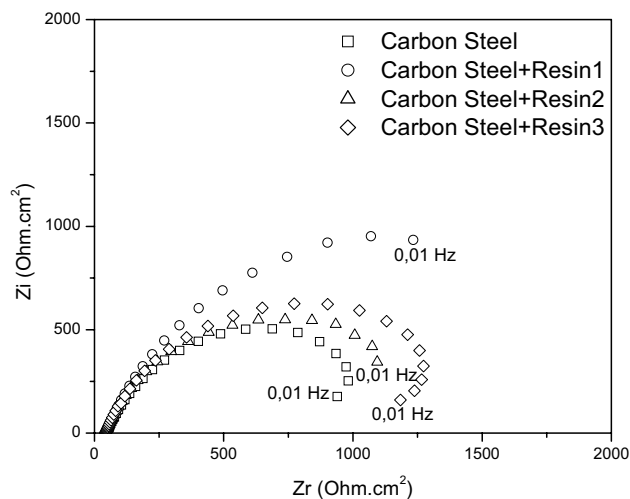


Fig. 9 Nyquist plots obtained in NaCl 0.5 mol L⁻¹ solution for bare and niobium-coated carbon steel (SAE 1020)

reaction, because there was a decrease of the current densities determined in the presence of the coatings.

The results demonstrate that niobium coating led to an increase in corrosion potential values, suggesting that, besides affecting the cathodic reaction, this coating also has a significant influence on the anodic reaction, as indicated in Figs. 7 and 8.

Corrosion rates (j_{corr}) were estimated by extrapolation of the linear segment of the cathodic curve to the corrosion potential. The average corrosion potential (E_{corr}) and (j_{corr}) values estimated from three measurements and also the corrosion inhibition efficiencies (θ) due to the phosphate layer are shown in Table 4.

The results presented in this table show that the niobium layer moves the E_{corr} into nobler values, suggesting that besides affecting the cathodic reaction it also influences the anodic reaction. It also shows that the efficiency associated with the niobium layer obtained from resin 1 is significantly superior to that of the layer formed in the other resin.

The EIS results obtained in NaCl 0.5 mol L⁻¹ solution are shown in Figs. 9 and 10 as Nyquist and impedance module plots. The Nyquist plots of the niobium-coated steels show a capacitive arc, suggesting a time constant.

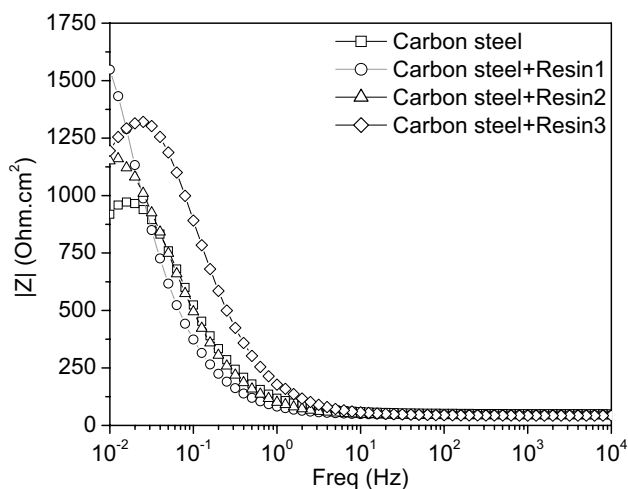


Fig. 10 Impedance module plot obtained in NaCl 0.5 mol L⁻¹ solution for bare and niobium-coated carbon steel (SAE 1020)

The Nyquist plots also show higher impedances associated with the coated samples compared to uncoated carbon steel. Coating had a significant effect on the impedance results, suggesting a delay in the charge transfer processes. Larger impedances were associated with carbon steel coated with niobium and demonstrated the higher corrosion resistance of coated steel. The oxide obtained with resin 1 provided higher corrosion resistance because it was more homogeneous. The EIS results supported the polarization measurements and indicated that the niobium layer was effective against corrosion.

The plots in Fig. 9 show an increase in the value of the impedance module $|Z|$ for samples coated with niobium resins. The increase in the value of $|Z|$ suggests the formation of a surface that is resistant to electrolytic solution attack. The sample with the highest value of $|Z|$ was that coated with resin 1, thus suggesting that this coating provides greater corrosion protection.

4 Conclusions

XRD analysis showed that the main phases in the niobium layers obtained with the three types of niobium resin used were NbO, NbO₂ and Fe_{0.998}Nb_{0.002}. The X-ray diffractograms show that the powder formed by the resin has an amorphous structure, but becomes crystalline in nature when applied on carbon steel.

The SEM micrographs showed that the niobium layer formed consists of crystals with a granular morphology that promotes surface coverage, leading to better corrosion resistance. The results also showed that the niobium coating obtained has a thickness of $14.93 \pm 0.997 \mu\text{m}$.

EDS analysis showed that there was a decrease in the amount of niobium in the coatings when the amount of ethylene glycol in the resins was increased.

Electrochemical characterization demonstrated a higher corrosion resistance associated with the coated substrate in comparison with the bare substrate. From the results of the present study, it can be concluded that niobium oxide layer can be used as a corrosion-protection coating for carbon steel.

Acknowledgements The authors are grateful for FUNDAÇÃO ARAUCÁRIA financial support provided to this research and also for CBMM for the Nb₂O₅ used in this study. This study was financed in part by the Coordenação de Aperfeiçoamento de Pessoal de Nível Superior—Brasil (CAPES)—Finance Code 001.

References

1. Roberge PR, Pierre R (1999) Handbook of corrosion engineering library of congress cataloging-in-publication data. Mac Graw-Hill, New York
2. Olivares-Navarrete R, Olaya JJ, Ramírez C (2011) Biocompatibility of niobium coatings. *Coatings* 1:72–87
3. Lima OJ, De Nassar EJ (2002) Testes de biocompatibilidade, aplicação e obtenção de novos materiais a partir do Nióbio. 25 Reunião Anual da Sociedade Brasileira de Química, vol 1, p 2–3
4. Yu J, Wen H, Shafiei M, Field MR, Liu ZF, Wlodarski W, Motta N, Li YX, Kalantar-Zadeh K, Lai PT (2013) A hydrogen/methane sensor based on niobium tungsten oxide nanorods synthesised by hydrothermal method. *Sens Actuators B* 184:118–129
5. Gong P, Palmiere EJ, Rainforth WM (2015) Dissolution and precipitation behaviour in steels microalloyed with niobium during thermomechanical processing. *Acta Mater* 97:392–403
6. Boukrība M, Sediri F (2014) Hydrothermal synthesis and characterization of poly(paraphenylenediamine)/Nb₂O₅ core-shell composite. *Ceram Int* 40:8499–8505
7. Kong F, Jiao G, Wang J, Tao S, Han Z, Fang Y, Yang G, Zhang L, Qian B (2017) Co-precipitation synthesis and electrochemical properties of CrNbO₄ anode materials for lithium-ion batteries. *Mater Lett* 196:335–338
8. Deblonde GJ, Chagnes A, Weigel V, Cote G (2016) Direct precipitation of niobium and tantalum from alkaline solutions using calcium-bearing reagents. *Hydrometallurgy* 165:345–350
9. Aegerter MA (2001) Sol-gel niobium pentoxide: a promising material for electrochromic coatings, batteries, nanocrystalline solar cells and catalysis. *Sol Energy Mater Sol Cells* 68(3–4):401–422
10. Martínez DT, Pérez RC, Delgado GT, Ángel OZ (2012) Structural, morphological, optical and photocatalytic characterization of ZnO–SnO₂ thin films prepared by the sol-gel technique. *J Photochem Photobiol A* 235:49–55
11. Graça MPF, Meireles A, Nico C, Valente MA (2013) Nb₂O₅ nano-size powders prepared by sol-gel—structure, morphology and dielectric properties. *J Alloys Compd* 553:177–182
12. Duta M, Predoana L, Calderon MJM, Preda S, Anastasescu M, Marin A, Dascalu I, Chesler P, Hornoiu C, Zaharescu M, Osiceanu P, Gartner M (2016) Nb-doped TiO₂ sol-gel films for CO sensing applications. *Mater Sci Semicond Process* 42:397–404
13. Lu Y, Khan S, Song CL, Wang KK, Yuan GZ, Li W, Han GR, Liu Y (2016) Doping concentration effects upon column-structured

- Nb:TiO₂ for transparent conductive thin films prepared by a sol-gel method. *J Alloys Compd* 663:413–418
14. Lazarova K, Vasileva M, Marinov G, Babeva T (2014) Optical characterization of sol-gel derived Nb₂O₅ thin films. *Opt Laser Technol* 58:114–118
 15. Viomar A, Maia GA, Scremin FR, Khalil NM, da Cunha MT, Antunes AC, Rodrigues PRP (2016) Influence of obtaining method of Nb₂O₅ particles used in dye sensitized solar cells consisting of TiO₂/Nb₂O₅. *Revista Virtual de Química* 8(3):889–900
 16. Rosario AV, Pereira EC (2006) The effect of composition variables on precursor degradation and their consequence on Nb₂O₅ film properties prepared by the Pechini method. *J Sol-Gel Sci Technol* 38(3):233–240
 17. Herval LKS, Dreifus von D, Rabelo AC, Rodrigues AD, Pereira EC, Gobato YG, Oliveira AJA, Godoy MPF (2015) The role of defects on the structural and magnetic properties of Nb₂O₅. *J Alloy Compd* 653:358–362
 18. Lustosa GMMM, Costa JPC, Perazolli LA, Stojanovic BD, Zaghete MA (2015) Electrophoretic deposition of (Zn, Nb)SnO₂-films varistor superficially modified with Cr³⁺. *J Eur Ceram Soc* 35(7):2083–2089
 19. Pechini M (1967) Method of preparing lead and alkaline earth titanates and niobates and coating method using the same to form a capacitor. US Patent 3,330,697
 20. Li W, Li J, Wang X, Ma J, Chen Q (2010) Effect of citric acid on photoelectrochemical properties of tungsten trioxide films prepared by the polymeric precursor method. *Appl Surf Sci*. <https://doi.org/10.1016/j.apsusc.2010.05.030>
 21. Graça MPF, Meireles A, Nico C, Valente MA (2013) Nb₂O₅ nanosize powders prepared by sol-gel-structure, morphology and dielectric properties. *J. Alloys Compd*. <https://doi.org/10.1016/j.jallcom.2012.11.128>
 22. Huízar-Félix AM, Hernández T, de la Parra S, Ibarra J, Kharisov B (2012) Sol-gel based Pechini method synthesis and characterization of Sm_{1-x}Ca_xFeO₃ perovskite 0.1 ≤ x ≤ 0.5. *Powder Technol* 229:290–293
 23. Martins ML, Florentino AO, Cavalheiro AA, Silva RIV, Dos Santos DI, Saeki MJ (2014) Mechanisms of phase formation along the synthesis of Mn-Zn ferrites by the polymeric precursor method. *Ceram. Int* 40:16023–16031
 24. Ribeiro PC, de Melo da Costa ACF, Kiminami RHGA, Sasaki JM, Lira HL (2013) Synthesis of TiO₂ by the pechini method and photocatalytic degradation of methyl red. *Mater Res* 16:468–472
 25. Trino LD, Dias LFG, Albano LGS, Bronze-Uhle ES, Rangel EC, Graeff CFO, Lisboa-Filho PN (2018) Zinc oxide surface functionalization and related effects on corrosion resistance of titanium implants. *Ceram Int* 44:4000–4008
 26. Costa M, Lira H (2014) Effect of calcination temperature on the structural characteristics and morphology of aluminas synthesized by the Pechini. *Materia* 19:171–182
 27. Raba AM, Bautista-Ruiz J, Joya MR (2016) Synthesis and structural properties of niobium pentoxide powders: a comparative study of the growth process. *Mater Res*. <https://doi.org/10.1590/1980-5373-MR-2015-0733>
 28. Orjuela GA, Rincón R, Olaya JJ (2014) Corrosion resistance of niobium carbide coatings produced on AISI 1045 steel via thermo-reactive diffusion deposition. *Surf Coat Technol* 259:667–675
 29. Fernandes FA, Gallego J, Picon CA, Tremiliosi Filho G, Casteletti LC (2015) Wear and corrosion of niobium carbide coated AISI 52100 bearing steel. *Surf Coat Technol* 279:112–117
 30. Nico C, Monteiro T, Graça MPF (2016) Niobium oxides and niobates physical properties: review and prospects. *J Prog Mater Sci* 80:1–37
 31. Galceran M, Pujol MC, Aguiló M, Díaz F (2007) Sol-gel modified Pechini method for obtaining nanocrystalline KRE(WO₄)₂ (RE = Gd and Yb). *J Sol-Gel Sci Technol* 42(1):79–88
 32. Tussolini M (2013) Caracterização das camadas de Nb₂O₅ na ausência ou presença de nanotubo de carbono e/ou carbetto de silício na superfície da liga de alumínio AA3003. Tese de Doutorado. Universidade Estadual do Centro Oeste
 33. Castillejo FE, Marulanda DM, Olaya JJ, Alfonso JE (2014) Wear and corrosion resistance of niobium-chromium carbide coatings on AISI D2 produced through TRD. *Surf Coat Technol* 254:104–111